Analysis of Multiple-Pulse Techniques under Fast MAS Conditions

C. Filip and S. Hafner*

*National R&D Institute for Isotopic and Molecular Technologies, P. O. Box 700, RO-3400 Cluj, Romania; and
Max-Planck Institut für Polymerforschung, P. O. Box 3148, D-55021 Mainz, Germany

The combination of magic-angle spinning and multiple-pulse sequences for line-narrowing in solids with homogeneous spin interactions is analyzed using Floquet theory. It is found that, for quasi-static conditions and for special synchronization conditions, line-narrowing is possible while for other conditions destructive interference of the two techniques takes place. However, even for optimum line-narrowing conditions, fundamental limitations with respect to the achievable linewidth are found, whereas the conditions of recoupling spin interactions are more easily realized. The implications of these results with respect to improving existing line-narrowing techniques or techniques for the design of specific Hamiltonians are discussed. © 2000 Academic Press

1. INTRODUCTION

One of the advantages of NMR spectroscopy with respect to other spectroscopy techniques is the relative ease by which the internal spin interactions can be manipulated in order to extract the information one is interested in. Important examples of such manipulation techniques are line-narrowing techniques such as multiple-pulse line-narrowing sequences (*1*) and magic-angle spinning (MAS) (*2, 3*). These techniques remove the anisotropic spin interactions that cause line-broadening in solids so that considerable resolution can be obtained. Apart from line-narrowing, multiple-pulse techniques become increasingly important also for designing particular forms of the spin-interaction Hamiltonians, for instance, for the generation of MQ coherences (*4, 5*).

The most convenient way to average anisotropic interactions is magic-angle spinning. By rotating the sample sufficiently fast at the so-called magic angle of 54.7° to the magnetic field, the space part of the anisotropic spin-interaction Hamiltonians is averaged out and the corresponding line-broadening vanishes. While this is fully true for inhomogeneous lines in the sense of Maricq and Waugh (*6*), e.g., for chemical-shift anisotropy, the situation is more difficult for so-called homogeneous interactions such as the multispin dipolar interaction. In this case, sufficient averaging is obtained only at high spinning speeds, i.e., when the spinning frequency exceeds the strongest dipolar coupling strength.

As was analyzed previously (*7*) based on a special Floquet formalism (*8*), the dipolar interaction behaves more and more

inhomogeneous-like for increasingly high spinning speeds. However, as a consequence of the homogeneous character a finite linewidth always remains. When investigating the linewidth as a function of the rotor frequency, it was derived that it behaves according to $1/\omega_R$ in the fast MAS limit (*7*). Considering the technical limitation related to the increase of the spinning frequency beyond the currently achievable frequency of 35 kHz, a considerable improvement in resolution by MAS alone thus cannot be expected in the near future.

Multiple-pulse line-narrowing techniques based on the averaging of the spin part of the interactions are an alternative to fast MAS. They are more efficient with respect to the line-narrowing of homogenous lines since the cycle time of these sequences can be usually made much shorter than the rotor period. Moreover, applying special symmetry conditions, high-order terms contributing to the linewidth can be eliminated (*9–11*). The main problem using multiple-pulse spectroscopy, however, is that pulses do not discriminate between the isotropic and the anisotropic (space) part of the interaction. That is, pulse sequences for eliminating chemical-shift anisotropy also remove the isotropic shift.

This limitation can be overcome by combining MAS and multiple-pulse sequences to so-called combined rotation and multiple-pulse spectroscopy (CRAMPS) experiments (*12–14*). In these experiments the multiple-pulse sequence is supposed to predominantly deal with the dipolar Hamiltonian, while the chemical-shift anisotropy is removed by sample spinning. It was, however, soon realized that both line-narrowing techniques interfere with each other when the characteristic time scales of the averaging processes are in the same order. In practice, CRAMPS experiments were thus confined to relatively slow MAS frequencies of 2–3 kHz. Such rotor speeds are not always sufficient for the removal of the chemical-shift anisotropy in the high magnetic fields of modern NMR spectrometers. This is one reason, among others, why nowadays high-speed MAS experiments are becoming increasingly popular (*5*).

The use of multiple-pulse sequences under the conditions of fast MAS was therefore investigated in previous papers (*15–17*). Two strategies for avoiding interference effects were found to be promising. Following the original CRAMPS ap-

proach, one can decouple both techniques using different time scales for the characteristic times of the two techniques. Under fast MAS, thus the cycle time of the pulse sequence must be reduced as much as possible leading to windowless or semi-windowless sequences (*15, 16*). The other approach (*17*) was to investigate special ratios of the cycle time t_c and the rotor period τ_R for which interference vanishes or is greatly reduced. Such synchronization conditions were established in zero-order approximation and a simple graphical scheme for the analysis of pulse sequences under MAS was developed (*5, 17*). While the treatment discussed above enables one to conveniently analyze necessary conditions for the design of pulse sequences, the limitation of this zero-order approach soon became evident. In particular for analyzing line-narrowing sequences, the homogeneous character is important, and a more accurate description is necessary. It is therefore the intention of this work to improve the treatment to the next order. After a brief experimental section to demonstrate the effect of interference on the line-narrowing efficiency, we will apply the Floquet approach discussed in (*7, 8*) to the case of multiple-pulse sequences.

2. EXPERIMENTAL

As motivation for the theoretical analysis following below, we now briefly investigate experimentally the limitations of multiple-pulse sequences under fast MAS as a function of the rotor frequency. The semi-windowless WHH-4 sequence of Refs. (*17, 16*) is used as an example. The experiments were performed on a Bruker ASX spectrometer with a standard Bruker 2.5-mm MAS probe allowing a maximum rotor frequency of 35 kHz. The pulse sequence according to (*16*) has been implemented with a 90° pulse length of 2 μs so that the total cycle time is 12 μs. For the acquisition of the signal, additional 4 μs are introduced after every pulse cycle following the strategy outlined in (*16*). The effective cycle time thus is increased toward 16 μs. L-Alanine was used as a test sample. Although the static linewidth of alanine extends 35 kHz (thus representing a real solid that cannot be dealt with by MAS alone), it can be conveniently narrowed using multiple-pulse sequences. Thus, alanine is an ideal sample for our purpose, the study of possible interference effects between pulse sequence and MAS.

For this study, the rotor frequency was varied in steps of 1 kHz between 10 kHz and the maximum of 35 kHz. Figure 1 shows selected multiple-pulse assisted MAS spectra for the rotor-frequency values of 10, 15, 20, 25, 27, 30, and 35 kHz. As can be seen from this selection, the influence of the rotor frequency is quite dramatic between 25 and 35 kHz, with a complete collapse of resolution at around 30 kHz.

For a more quantitative analysis, the residual linewidths have been evaluated. Figure 2 shows the resulting linewidth of the CH$_3$ peak of the multiple-pulse assisted MAS spectrum as a function the scaled rotor frequency t_c/τ_R. In the low-fre-
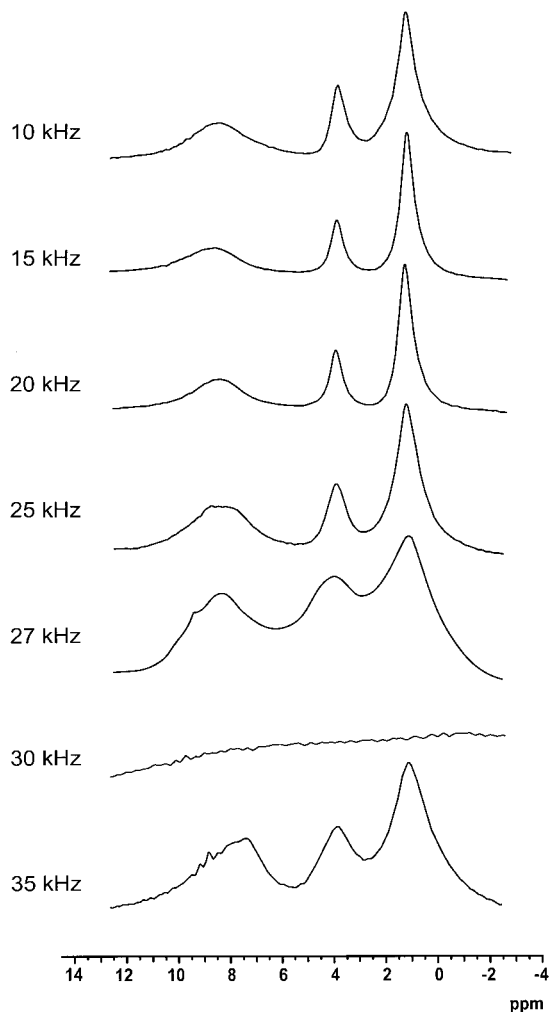

FIG. 1. Selected multiple-pulse assisted MAS spectra of L-alanine acquired at the rotor frequencies specified to the left. With the exception of the baseline-like spectrum at 30 kHz, the spectra have been normalized to the same peak high of the strongest peak (CH$_3$ peak). The interference between MAS and the WHH-4 pulse sequence can be estimated by the corresponding line broadening. For more details on the experiment see Section 2.

quency part, the linewidth decreases with increasing rotor frequency. In this range, MAS increasingly contributes to the elimination of line-broadening effects resulting from misadjustments, hardware limitations, and the error terms of the WHH-4 sequence.

At around 12–13 kHz—still in the quasi-static regime—a plateau is obtained which ranges up to 22 kHz. The upper value corresponds to around $t_c/\tau_R = \frac{1}{3}$ which, according to zero-order theory, is a condition of decoupling between the two line-narrowing techniques. That is, the plateau ranges from quasi-static conditions up to the synchronization range without displaying any influence of zero-order synchronization conditions such as $t_c/t_R = \frac{1}{3}, \frac{1}{4}, \frac{1}{5}$, and so on. These conditions are obviously washed out by the influence of
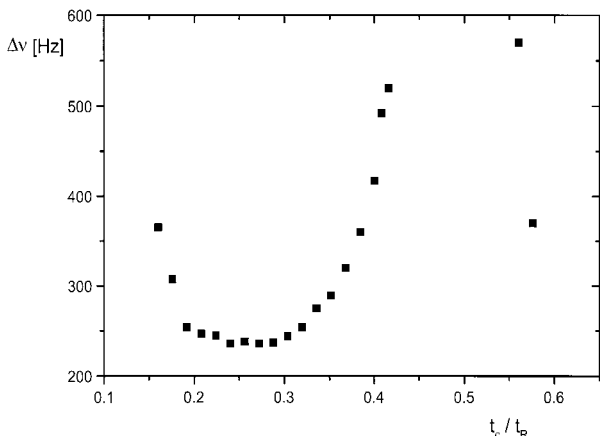
FIG. 2. Residual linewidths of the CH$_3$ lines as a function of the scaled rotor frequency t_c/τ_R (t_c is the cycle time of the pulse sequence and τ_R is the rotor period) for the series of multiple-pulse assisted MAS spectra of L-alanine. For low values of the rotor frequency, the linewidth is decreasing due to the increasingly stronger averaging by MAS until at around $t_c/\tau_R = 0.2$ a plateau is reached. At around $t_c/\tau_R = 0.3$ interference effects start to dominate and lead to an increase of the linewidth. At the first recoupling condition $t_c/\tau_R = 0.5$ the recoupling is so strong that the linewidth cannot be determined anymore. For higher rotor frequencies, the linewidth then decreases again until finally the maximum spinning frequency of 35 kHz is reached.

higher order terms, that is, they seem to merge with each other and with the quasi-static limit.

Reasons for line-broadening in this range are probably error terms of the pulse sequence that are not fully removed, instrumental imperfections that cannot be completely dealt with by fast MAS (for instance B_1 inhomogeneities), and contributions due to the interference of the two techniques (i.e., due to the failure of the quasi-static approximation). Nevertheless, resolution in this range is much better than that found in MAS-alone spectra (not shown) where the CH and CH$_3$ groups are still not resolved. As usual in multiple-pulse NMR, the importance of the different contributions is difficult to judge. Qualitatively, one would assume that the interference effects do not dominate in the plateau because they are supposed to strongly depend on the rotor frequency.

At around 20 kHz the effects of synchronization start to become important. Above 27 kHz, close to the recoupling condition $t_c/\tau_R = \frac{1}{2}$, the linewidth becomes even too large to be measurable (merger of the three lines) while the MAS-alone linewidth now is below 1 kHz for the CH$_3$ group. Finally, starting at around 34–35 kHz, the lines of the multiple-pulse spectra become resolved again.

Summarizing these findings, one can state that the interpretation of the results on the basis of zero-order theory are not satisfactory since most of the predicted synchronization conditions are washed out by the homogeneous nature of the interactions, which is not accounted for in this approximation. A more detailed analysis that includes the homogeneous parts of the interactions is thus necessary.

3. THEORY

3.1. General Approach

Floquet theory is a powerful tool for the treatment of experiments under MAS (*18–21*). An analytical Floquet formalism that is particularly suitable for our purpose was developed in Ref. (*8*). It can be applied to a general rotor modulated Hamiltonian

$$\mathcal{H}(t) = \sum_{m=-2}^{2} e^{im\omega_R t} \mathcal{H}_m, \qquad [1]$$

regardless of the particular form of the isotropic ($\mathcal{H}_0$) and anisotropic ($\mathcal{H}_m$, $m = \pm 1, \pm 2$) components. The spectral separation and the residual broadening of the NMR lines inside of each MAS sideband are then conveniently described by the effective Hamiltonian

$$\mathcal{H}_{\text{eff}} = \mathcal{H}_0 + \sum_m \frac{[\mathcal{H}_m, \mathcal{H}_{-m}]}{2m\omega_R} + \cdots. \qquad [2]$$

When MAS is combined with cyclic multiple-pulse sequences, the interaction Hamiltonian, Eq. [1], acquires a double time periodicity,

$$\mathcal{H}(t) = \sum_{m=-2}^{2} e^{im\omega_R t} \mathcal{H}_m(t), \qquad [3]$$

since here also the Fourier components $\mathcal{H}_m$ are periodically time-dependent with the cycle time t_c of the given multiple-pulse sequence.

Two cases of pulsed line-narrowing techniques are to be distinguished now, the Lee–Goldburg-type sequences (*22*) where (similar to MAS in the real space) the periodicity introduced by the radiofrequency is continuous, and conventional multiple-pulse sequences were the $\mathcal{H}_m(t)$ are discontinuous functions of time (*1, 9–11*). In the first case, a double Floquet treatment appears to be convenient, while in the second the use of Floquet theory for both modulations is no more advantageous. Separate treatments for the two cases, however, can be avoided by noting that in any case the data are acquired only at multiples of the cycle time. Thus, the much simpler average Hamiltonian treatment (*1, 11*) can be employed for both cases, disregarding the detailed spin dynamics between two acquisition points.

For simplicity, we thus confine our study, without loss of generality, to the case of a conventional multiple-pulse sequence. In order to bring the double time-periodic Hamiltonian, Eq. [3], to a form similar to that of Eq. [1], an average over t_c first has to be made. Since the periodicity with t_c is

determined by the multiple-pulse sequence, we employ the Magnus expansion (23) to replace the time-dependent $\mathcal{H}_m(t)$ with time-independent Fourier components. Unlike the treatment of a static sequence, however, here the time-variation induced by MAS is also taken into account. For the averaging, we consider the general expression of a k order term in the Magnus expansion,

$$\bar{\mathcal{H}}^{(k)}(n) \sim \int_{nt_c}^{(n+1)t_c} e^{im_k\omega_R t_k} dt_k \int_{nt_c}^{t_k} e^{im_{k-1}\omega_R t_{k-1}} dt_{k-1} \cdots$$
$$\int_{nt_c}^{t_2} e^{im_1\omega_R t_1} dt_1 F(\mathcal{H}_{m_k}(t_k), \ldots, \mathcal{H}_{m_1}(t_1)), \qquad [4]$$

corresponding to an arbitrary cycle n inside a given multiple-pulse sequence, that is, within the time interval $[nt_c, (n+1)t_c]$.

The form of the function $F(\mathcal{H}_{m_k}(t_k), \ldots, \mathcal{H}_{m_1}(t_1))$ is not relevant for the present discussion since it does not explicitly depend on time. Substituting $t'_k \rightarrow t_k - nt_c$, $t'_{k-1} \rightarrow t_{k-1} - nt_c$, $\ldots$, $t'_1 \rightarrow t_1 - nt_c$, Eq. [4] transforms to

$$\bar{\mathcal{H}}^{(k)}(n) \sim e^{i(m_k+m_{k-1}+\cdots+m_1)\omega_R(nt_c)}$$
$$\times \int_0^{t_c} e^{im_k\omega_R t'_k} dt'_k \int_0^{t'_k} e^{im_{k-1}\omega_R t'_{k-1}} dt'_{k-1} \cdots$$
$$\int_0^{t'_2} e^{im_1\omega_R t'_1} dt'_1 F(\mathcal{H}_{m_k}(t'_k), \ldots, \mathcal{H}_{m_1}(t'_1))$$
$$= e^{i(m_k+m_{k-1}+\cdots+m_1)(nt_c)} \bar{\mathcal{H}}^{(k)}(0). \qquad [5]$$

The factor obtained after integration is independent of n although the modulation by MAS is included in the integral $\bar{\mathcal{H}}^{(k)}(0)$. It characterizes the "internal structure" of the multiple-pulse sequence through t_c and $\mathcal{H}_{m_k}(t'_k)$. The time-dependence by MAS is expressed in Eq. [5] by the modulation factor $\exp[im\omega_R(nt_c)]$, ($m = m_k + m_{k-1} + \cdots + m_1$), which now depends on the "position" on the time axis of the considered cycle n. Thus, the average Hamiltonian $\bar{\mathcal{H}}^{(k)}(n)$ of an arbitrary cycle n can be expressed by the average Hamiltonian of the first cycle $\bar{\mathcal{H}}^{(k)}(0)$ and a phase factor $\exp[im\omega_R(nt_c)]$ that represents its position on the time axis of the experiment. It is important to emphasize here that, although the above result is valid only at discrete moments of time $t = nt_c$, in practice a continuously running time t can be assumed since the observation windows are located at integer multiples of the cycle time.

Since the above considerations apply to any order in the Magnus expansion, we finally find that Eq. [3] can be rewritten in a form similar to that of the MAS Hamiltonian Eq. [1], i.e.,

$$\mathcal{H}(t) = \sum_{m=-2}^{2} e^{im\omega_R t} \bar{\mathcal{H}}_m. \qquad [6]$$

The Fourier components $\bar{\mathcal{H}}_m$ are expressed now through a Magnus expansion, $\bar{\mathcal{H}}_m = \bar{\mathcal{H}}_m^{(0)} + \bar{\mathcal{H}}_m^{(1)} + \cdots$. The remaining rotor modulation can be removed as in the case of MAS-alone experiments, employing the procedure described in (7). Confining the study to the part which is responsible for residual broadening, one thus can conclude that the combined effects of MAS and the applied multiple-pulse sequence can be characterized by an effective Hamiltonian of the form of Eq. [2], i.e.,

$$\bar{\mathcal{H}}_{eff} = \bar{\mathcal{H}}_0 + \sum_m \frac{[\bar{\mathcal{H}}_m, \bar{\mathcal{H}}_{-m}]}{2m\omega_R} + \cdots, \qquad [7]$$

where the Fourier components $\mathcal{H}_m$ are replaced by the averaged components $\bar{\mathcal{H}}_m$.

We consider now a general multiple-pulse sequence with cycle time t_c that is composed of N different time intervals τ_α (with $\alpha = 1, \cdots, N$). During each of these intervals, the spin interactions are represented by a toggling-frame Fourier component $H_{\alpha,m}$. In Eq. [3] one thus has to set $\mathcal{H}_m = H_{1,m}$ for $nt_c < t < nt_c + \tau_1, \cdots, \mathcal{H}_m = H_{N,m}$ for $nt_c + \tau_1 + \cdots + \tau_{N-1} < t < (n+1)t_c$. For simplicity we confine our study to the δ-pulse approximation, although in some of the experiments under fast MAS a semi-windowless limit is actually used. The treatment of the semi-windowless sequence, however, gives only additional terms (crossterms) that would lead to complications without providing much new insight. Applying the above procedure up to the first-order terms in the Magnus expansion, one obtains

$$\bar{\mathcal{H}}_0^{(0)} = \frac{1}{t_c} \sum_\alpha H_{\alpha,0}\tau_\alpha$$
$$\bar{\mathcal{H}}_m^{(0)} = \frac{1}{t_c} \sum_\alpha c_m(\tau_\alpha) H_{\alpha,m}, \qquad [8]$$

with

$$c_m(\tau_\alpha) = e^{im\omega_R(\tau_1+\cdots+\tau_{\alpha-1})} \frac{e^{im\omega_R\tau_\alpha} - 1}{im\omega_R} \qquad [9]$$

and

$$\bar{\mathcal{H}}_0^{(1)} = \frac{-i}{2t_c} \sum_m \{ \sum_{\beta>\alpha} c_m(\tau_\beta)c_{-m}(\tau_\alpha)[H_{\beta,m}, H_{\alpha,-m}]$$
$$+ \sum_\alpha c_{0,m}(\tau_\alpha)[H_{\alpha,m}, H_{\alpha,-m}] \}$$

$$\bar{\mathscr{H}}_m^{(1)} = \left(\frac{-i}{2t_c}\right)^{p+q=m} \sum_{p,q} \left\{ \sum_{\beta>\alpha} c_p(\tau_\beta)c_q(\tau_\alpha)[H_{\beta,p}, H_{\alpha,q}] \right.$$
$$\left. + \sum_\alpha c_{p,q}(\tau_\alpha)[H_{\alpha,p}, H_{\alpha,q}] \right\}, \qquad [10]$$

with

$$c_{p,q}(\tau_\alpha) = \frac{1}{iq\omega_R}\left(c_{p+q}(\tau_\alpha) - e^{iq\omega_R(\tau_1+\cdots+\tau_{\alpha-1})}c_p(\tau_\alpha)\right) \quad [11]$$

and

$$c_{0,m}(\tau_\alpha) = \frac{1}{im\omega_R}\left(c_m(\tau_\alpha) - e^{iq\omega_R(\tau_1+\cdots+\tau_{\alpha-1})}\tau_\alpha\right). \quad [12]$$

3.2. Specific Example

The treatment so far is still general since neither the spin system nor the pulse sequence is specified. To keep the analysis simple, we now confine our study to the WHH-4 pulse sequence (*1*). The treatment of this specific example may then serve as a guideline for the analysis of any other multiple-pulse sequence. That is, we are not so much interested in this specific sequence but in studying the general aspects of such experiments on this example. In the following we thus concentrate on the results and refer the interested reader to the Appendix for details of the calculation.

Applying Eqs. [7]–[12] to the particular conditions of the WHH-4 pulse sequence and restricting the analysis to the first-order terms of the effective Hamiltonian, Eq. [7], one obtains (see Appendix)

$$\bar{\mathscr{H}}_{eff} = \bar{\mathscr{H}}_{eff}^{(0)} + \bar{\mathscr{H}}_{eff}^{(1)} \qquad [13]$$

with

$$\bar{\mathscr{H}}_{eff}^{(0)} = \frac{1}{3}\sum_i \omega_i(I_{ix} + I_{iy} + I_{iz}) \qquad [14]$$

and

$$\bar{\mathscr{H}}_{eff}^{(1)} = \bar{\mathscr{H}}_0^{(1)} + \sum_m \frac{[\bar{\mathscr{H}}_m^{(0)}, \bar{\mathscr{H}}_{-m}^{(0)}]}{2m\omega_R}$$
$$= \sum_m \left\{ f_m(\tau) \sum_{\alpha,\beta} f_m^{\alpha\beta}(\tau) \frac{[H_{\alpha,m}^D, H_{\beta,-m}^D]}{2m\omega_R b} \right.$$
$$\left. + g_m(\tau) \frac{[F_m^D, F_{-m}^D]}{2m\omega_R} \right\}. \qquad [15]$$

Here, ω_i is the isotropic chemical shift of the ith nucleus and α, β run over x, y, and z. $H_{\alpha,m}^D = \sum_{j>i} \omega_m^{(ij)}(\theta_{ij}, \varphi_{ij})(3I_{i\alpha}I_{j\alpha} - \mathbf{I}_i\mathbf{I}_j)$ is the α component of the full dipolar Hamiltonian, while $F_m^D = \sum_{j,k} b_m^{ij}(\theta_{ij}, \varphi_{ij})\mathbf{I}_j\mathbf{I}_k$ represents its isotropic part (with respect to the spin operators). The coefficients $g_m(\tau)$ and $f_m(\tau)$ represent those parts of what we call synchronization functions that are independent of (α, β). They are derived in the Appendix as

$$f_m(\tau) = \frac{2\pi}{3}\frac{1 - \cos(m\omega_R\tau)}{m\omega_R\tau} \qquad [16]$$

and

$$g_m(\tau) = \frac{1}{6}\left(1 - \frac{\sin(m\omega_R\tau)}{m\omega_R\tau}\right). \qquad [17]$$

Those parts of the synchronization functions that depend on (α, β) are also derived in the Appendix and are given by

$$f_m^{xx}(\tau) = 2\left[\sin\left(\frac{5}{2}m\omega_R\tau\right) + \frac{1}{3m\omega_R\tau}\cos\left(\frac{5}{2}m\omega_R\tau\right)\right]$$
$$\times \cos\left(\frac{5}{2}m\omega_R\tau\right)$$

$$f_m^{yy}(\tau) = 2\left[\sin\left(\frac{3}{2}m\omega_R\tau\right) + \frac{1}{3m\omega_R\tau}\cos\left(\frac{3}{2}m\omega_R\tau\right)\right]$$
$$\times \cos\left(\frac{3}{2}m\omega_R\tau\right)$$

$$f_m^{zz}(\tau) = 2\left[\sin\left(\frac{1}{2}m\omega_R\tau\right) + \frac{1}{3m\omega_R\tau}\cos\left(\frac{1}{2}m\omega_R\tau\right)\right]$$
$$\times \cos\left(\frac{1}{2}m\omega_R\tau\right)$$

$$f_m^{xy}(\tau) = 2\left[\sin\left(\frac{5}{2}m\omega_R\tau\right) + \frac{1}{3m\omega_R\tau}\cos\left(\frac{5}{2}m\omega_R\tau\right)\right]$$
$$\times \cos\left(\frac{3}{2}m\omega_R\tau\right)$$

$$f_m^{xz}(\tau) = 2\left[\sin\left(\frac{5}{2}m\omega_R\tau\right) + \frac{1}{3m\omega_R\tau}\cos\left(\frac{5}{2}m\omega_R\tau\right)\right]$$
$$\times \cos\left(\frac{1}{2}m\omega_R\tau\right)$$

$$f_m^{yz}(\tau) = 2\left[\sin\left(\frac{3}{2}m\omega_R\tau\right) + \frac{1}{3m\omega_R\tau}\cos\left(\frac{3}{2}m\omega_R\tau\right)\right]$$
$$\times \cos\left(\frac{1}{2}m\omega_R\tau\right). \qquad [18]$$

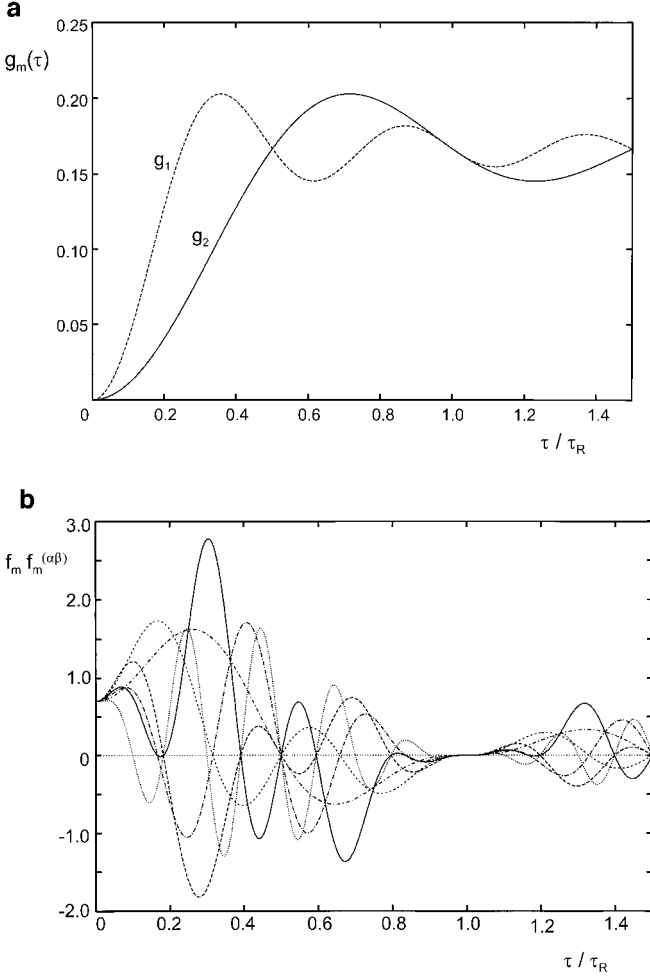**FIG. 3.** (a) The synchronization functions $g_m(\tau)$, Eq. [36], for both Fourier indices $m = 1$, 2 as a function of τ/τ_R (τ is the pulse length of the semi-windowless WHH-4 sequence—see Experimental). (b) The same plot for the six synchronization functions $f_m(\tau)f_m^{(\alpha\beta)}(\tau)$, Eqs. [35] and [18], that result from all possible combinations α, $\beta = x$, y, and z; here only $m = 1$ was considered.

Figure 3a shows a plot of the functions $g_m(\tau)$ and Fig. 3b of $f_m(\tau)f_m^{\alpha\beta}(\tau)$. On this basis we are able now to discuss interference and synchronization.

3.3. Synchronization

For discussing the line-narrowing efficiency of multiple-pulse techniques under MAS conditions we rely on the results obtained for the WHH-4 sequence but the conclusions drawn on this basis are more generally valid. As in the case of fast MAS (7) and of multiple-pulse sequences (1, 11) alone, here also the line-narrowing is primarily due to the removal of two-spin correlations from $\bar{\mathcal{H}}_{\text{eff}}$. The way, however, in which the remaining spin correlations contribute to the residual broadening is different since each order in the power expansion of $\bar{\mathcal{H}}_{\text{eff}}$ contains the effects of both MAS and the applied

multiple-pulse sequence. The ideal situation is given when the two techniques are completely decoupled from each other: in this case, the lowest order terms would be eliminated, for instance, by the action of the multiple-pulse sequence while the higher order terms are greatly reduced by fast spinning. However, as will be shown below, there is a strong interference between MAS and the multiple-pulse sequence, and only for some special conditions is decoupling approached but never fully reached in practice.

To demonstrate this, we consider the results obtained in the previous section. The zero-order term of the effective Hamiltonian, Eq. [7], corresponds to the scaled isotropic chemical shift. Therefore, at this level there is no interference between sample rotation and pulse sequence. Interference starts to appear only with the first order. Comparing Eq. [15] with the first-order term of the MAS-alone case,

$$\mathcal{H}_{\text{eff}}^{(1)} = \frac{[H_{z,m}^{\text{D}}, H_{z,-m}^{\text{D}}]}{2m\omega_{\text{R}}}, \qquad [19]$$

one can identify the following effects that are responsible for interference: (i) the original (z, z) component of the MAS-alone case (see commutator in Eq. [19]) splits into all possible (α, β) components (see Eq. [15]), and the relative contributions of each of the components to the resulting Hamiltonian are weighted by synchronization functions $f_m(\tau)f_m^{\alpha\beta}(\tau)$, and (ii) there is an additional term in Eq. [15] that represents the isotropic contribution with respect to the spin operators, as already discussed.

The two narrowing techniques act independently of each other if the first-order term given by Eq. [15] is eliminated. This translates into following conditions for the synchronization functions: $g_m(\tau) = 0$ and $f_m(\tau) \cdot f_m^{\alpha\beta}(\tau) = \text{const.} = A_m$ simultaneously for both Fourier components, $m = 1$, 2. In this case, Eq. [15] transforms to

$$\bar{\mathcal{H}}_{\text{eff}}^{(1)} \sim \sum_m A_m \frac{[H_{x,m}^{\text{D}} + H_{y,m}^{\text{D}} + H_{z,m}^{\text{D}}, H_{x,-m}^{\text{D}} + H_{y,-m}^{\text{D}} + H_{z,-m}^{\text{D}}]}{2m\omega_{\text{R}}} = 0. \qquad [20]$$

Thus, $\bar{\mathcal{H}}_{\text{eff}}^{(1)}$ vanishes due to the magic-zero condition of the dipolar interaction $H_{x,m}^{\text{D}} + H_{y,m}^{\text{D}} + H_{z,m}^{\text{D}} = 0$, that is, due to the action of the WHH-4 pulse sequence which, under these conditions, does not interfere with MAS.

As can be seen from Figs. 3a and 3b, the above requirements can be fulfilled only for a limited number of cases. More specifically, $g_m(\tau)$ is exactly zero only when the ratio $\tau/\tau_R \sim \omega_R\tau$ equals zero (see Fig. 3a), that is, when the (quasi-)static regime is ideally fulfilled. The other relation, $f_m(\tau) \cdot f_m^{\alpha\beta}(\tau) = A_m$, holds if $\tau/\tau_R = k/2m$ for $m = 1$ and 2 and $k = 0$, 1, 2 ... The case of $m = 1$ is illustrated in Fig. 3b, where all six synchronization functions are shown. For $m = 2$ everything is

similar except that the τ/τ_R-axis is "compressed" by a factor of two. Therefore, in this case the values $\tau/\tau_R = k/4$ ($k = 0, 1, 2 \ldots$) satisfy the above requirement.

As long as none of the functions $f_m(\tau) \cdot f_m^{\alpha\beta}(\tau) = A_m$ and $g_m(\tau)$ can be neglected, the above conditions are fully satisfied only when τ/τ_R is close to zero, that is, for the (quasi-)static case. In this case, $g_m(\tau)$ approaches zero (Fig. 3a) while the synchronization functions $f_m(\tau) \cdot f_m^{\alpha\beta}(\tau)$ are close to each other (Fig. 3b). Then, $\tilde{\mathcal{H}}_{eff}^{(1)}$ can be very well neglected, MAS and the applied multiple-pulse sequence act almost independently, and decoupling is fully achieved. However, one should note that in practice quasi-static conditions are difficult to be obtained outside of the classical CRAMPS limit (slow spinning at around 2 kHz). In the case of multiple-pulse assisted MAS experiments where sufficiently fast MAS is supposed to contribute to decoupling, a compromise must be found between the cycle time of the applied pulse sequence and the achievable spinning speed.

From this point of view, the synchronized cases ($\tau/\tau_R = k/2$) with $k > 0$ appear to be more advantageous since they are well compatible with the fast spinning regime. Moreover, in principle, they can be exactly fulfilled for a rotating sample while the other condition ($k = 0$) is exactly valid only for the static case. A drawback of this approach, however, is that the synchronization condition $\tau/\tau_R = k/2$ leads to very large dwell times: even in the most favorable case ($\tau/\tau_R = \frac{1}{2}$ and a maximum rotor frequency of 35 kHz) the corresponding dwell time, $\delta t = 3\tau_R \simeq 100 \ \mu s$, is so large that there might be problems with the spectral width in the case of off-resonance acquisition (which is mostly used in multiple-pulse experiments). Another, more principal, problem is the second term in $\tilde{\mathcal{H}}_{eff}^{(1)}$ which cannot be made zero by synchronization (see Fig. 3a). However, since it is scaled by the comparatively small values of $g_m(\tau)$ (compare Fig. 3a with Fig. 3b), it can be neglected in first approximation.

Inspecting Fig. 3b again, the τ/τ_R range for some of the decoupling conditions is very narrow, for instance, for $\tau/\tau_R = \frac{1}{2}$. Apart from the difficulty in adjusting such narrow conditions, it is not clear how much the close neighborhood of recoupling conditions affects the achievable resolution in these cases. More generally, outside of special synchronization conditions, one can no longer judge the narrowing efficiency by simply qualitatively inspecting the synchronization functions $f_m(\tau) \cdot f_m^{\alpha\beta}(\tau)$. Their behavior gets extremely complicated as we move away from the special points $\tau/\tau_R = k/2$ (see Fig. 3b). To further analyze the linewidth in these cases one can use a more quantitative approach based on the second moment analysis.

3.4. Linewidth and Second Moment

The residual linewidth is related to the second moment according to $\Delta\nu \sim \sqrt{M_2}$ (see also (7)). The contribution of the dipolar interaction to the second moment is in our case given by
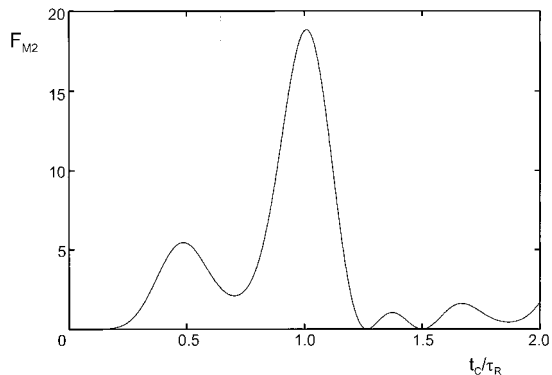

FIG. 4. Scaling function F_{M2} according to Eq. [24] as a function of t_c/τ_R. This function represents the influence of interference effects on the residual linewidths. The plot thus can be taken as a qualitative representation of the linewidth as a function of t_c/τ_R. The range corresponding to the experiment (see Fig. 2) is indicated by two dotted lines.

$$M_2 \sim \langle I_y | \mathcal{H}_{eff}^{(1)2} | I_y \rangle. \tag{21}$$

For the estimation of the second moment we should take into account that the (α, α) components in Eq. [15] are related to each other through $\sum H_{\alpha,m}^D = -3F_m^D$. One can further simplify the analysis assuming that all spins have approximately the same isotropic chemical shifts. Then, the commutation properties $[F_{ij,m}^D, I_{i\alpha} + I_{j\alpha}] = 0$ and $[H_{y,m}^D, I_{iy} + I_{jy}] = 0$ hold so that the second moment depends only on the (z, z) dipolar Hamiltonian as in the case of MAS alone. Thus, the final expression,

$$M_2 = \sum_{m,p} M_2^{MAS} \mathcal{F}_m(\tau) \mathcal{F}_p(\tau), \tag{22}$$

contains the moment M_2^{MAS} of the MAS-alone case scaled by the functions

$$\mathcal{F}_m(\tau) = f_m(\tau)[f_m^{xx}(\tau) - f_m^{zz}(\tau)]. \tag{23}$$

Here, we have assumed that all terms with different Fourier indices contribute equally to the second moment, while in reality the contribution depends on the arrangement of spins in the investigated system. However, this affects only the absolute value of M_2 for a given spin system but not the qualitative behavior of M_2 as a function of t_c/τ_R.

Figure 4 shows the scaling function of the second moment

$$F_{M2} = \sum_{m,p} \mathcal{F}_m(\tau) \mathcal{F}_p(\tau) \tag{24}$$

as a function of t_c/τ_R. This function represents the influence of interference effects relative to the MAS-only second moment, M_2^{MAS}. It should be noted that M_2^{MAS} is not a constant but a decreasing function of the rotor frequency. For our qualitative

considerations, however, we can disregard this since linewidth changes caused by interference are exclusively represented by the scaling function F_{M2}.

By inspecting Fig. 4, one can identify "partial synchronization" windows, where M_2 (represented by F_{M2}) is comparatively small (decoupling case), and windows of strong destructive interference where the opposite applies (recoupling case). Qualitatively, this result agrees well with the measured curve. In particular, it can be seen in Fig. 4 that the distinct synchronization conditions expected from zero-order theory are smoothed out as is indeed found experimentally. Further, it can be seen that full decoupling is not possible between the two first recoupling conditions $t_c/\tau_R = 0.5$ and $t_c/\tau_R = 1$. On the other hand there are two conditions of full decoupling at around $t_c/\tau_R = 1.3$ and $t_c/\tau_R = 1.5$.

A strong deviation between theory and experiment is found in the low-frequency range up to about 10 kHz where the experimental lines are relatively broad, although quasi-static conditions are quite well fulfilled in this regime. However, as already discussed, the experimental performance of the applied pulse sequence (which is not high-order compensated) is relatively modest and cannot be fully compensated by MAS at such low rotor frequencies. Only at frequencies above 10 kHz is MAS able to sufficiently average the remaining terms ($\sim 1/\omega_R^2$, $1/\omega_R^3$, ...) in the power expansion of $\bar{\mathscr{H}}_{\text{eff}}^{(1)}$ [7].

If one compares the experimental result and the theory more closely, there are some small differences in the shape of the recoupling peak at $t_c/\tau_R = \frac{1}{2}$, which seems to be sharper in Fig. 2 than in Fig. 4. Here one should keep in mind that the decrease of the MAS-only moment with the rotor frequency is not accounted for by the scaling function F_{M2} while it contributes to the experimental data. Apart from that, some deviations between theory and experiment are not unexpected, considering the various simplifications made for the derivation of Eqs. [22] and [23]. In particular, the treatment is valid only in first order and the δ-pulse approximation has been used while actually the opposite, a semi-windowless sequence, was applied experimentally.

3.5. Evolution of Coherences

So far, we have concentrated on the effective Hamiltonian $\bar{\mathscr{H}}_{\text{eff}}$ which is usually sufficient for describing line-narrowing experiments. For the analysis of other multiple-pulse experiments performed under MAS such as multiple-quantum experiments, however, the whole time evolution might be of interest including those contributions that are refocused by MAS for full rotor periods [5]. Then, it is not sufficient to consider only the effective Hamiltonian; the full propagator must be analyzed.

This analysis can be made by extending the results that have been derived in [8] for studying simple one-pulse MAS experiments. For this, a general expression of the MAS time propagator between two arbitrary moments of time, t_1 and t_2, is required. Such a generalization is easily made following the procedure developed in [8]. The only difference is that now the

initial state is not defined at $t = 0$ but at a time t_1 so that the initial state $\rho(t_1)$ already incorporates the influence of MAS. The result finally obtained for the general MAS propagator is

$$\hat{U}_{\text{MAS}}(t_2, t_1)$$
$$= \sum_{m_j} e^{m_j \omega_R t_2} \hat{C}^\dagger(-m_j) e^{-i\hat{\mathscr{H}}_{\text{eff}}(t_2-t_1)} \sum_{m_k} e^{m_k \omega_R t_1} \hat{C}(m_k). \quad [25]$$

The coefficients $\hat{C}(m)$ represent the refocused part and are important for experiments where sideband analysis is of interest. Both these coefficients and the effective Hamiltonian $\mathscr{H}_{\text{eff}}$ are given by power expansions in $1/\omega_R$ (see Ref. [8] for the explicit form).

For the treatment of combined MAS and multiple-pulse experiments, we apply Eq. [6] to the propagator, Eq. [25], which then transforms to

$$\widehat{\bar{U}}_{\text{MAS}}(t_2, t_1)$$
$$= \sum_{m_j} e^{m_j \omega_R t_2} \widehat{\bar{C}}^\dagger(-m_j) e^{-i\widehat{\bar{\mathscr{H}}}_{\text{eff}}(t_2-t_1)} \sum_{m_k} e^{m_k \omega_R t_1} \widehat{\bar{C}}(m_k). \quad [26]$$

The result is of the same form as Eq. [25] only with the coefficients and the effective Hamiltonian replaced by their averaged symbols. In analogy to the effective Hamiltonian $\bar{\mathscr{H}}_{\text{eff}}$, the coefficients $\widehat{\bar{C}}(m)$ can be found by replacing the bare Fourier components $\mathscr{H}_m$ with the averaged components $\bar{\mathscr{H}}_m$ in the corresponding expressions. An important consequence of Eq. [26] is that the formalism developed in the previous sections is more generally applicable. It is not only useful for deriving the effective Hamiltonian, Eq. [7], but in fact the full-time propagator, Eq. [26], can be handled. That is, in principle, it can be employed to any cyclic pulse NMR experiment under MAS.

4. DISCUSSION AND CONCLUSIONS

In the present work we have developed a theoretical treatment that is generally applicable for the description of multiple-pulse sequences under MAS. It is based on a combination of average Hamiltonian theory as a well-established tool for the analysis of multiple-pulse sequences [1, 23, 24] and Floquet theory [8, 18–21] for treating spin dynamics in rotating solids.

A special analytical Floquet formalism has been used [8] that has been already applied for the study of (homogeneous) spin interactions under MAS [7]. The advantage of this formalism with respect to the above analysis is that the MAS time propagator and the pulse propagator $\hat{U}_{\text{av}} = \exp[-i\hat{\mathscr{H}}(t_2 - t_1)]$ both act within the same Liouville (or Hilbert) space while in other Floquet treatments an infinite-dimensional Floquet–Hilbert space is used for describing MAS [18–21]. Moreover, as already stated in previous work [7, 8], this Floquet formalism allows various aspects of a given MAS experiment to be conveniently interpreted, such as, for example, the rotor-fre-

quency dependence of relevant parameters. The fundamental result of combining average Hamiltonian theory and Floquet theory is expressed by Eqs. [5] and [6], which thus can be taken as a basis for analyzing any multiple-pulse sequence under MAS.

The main motivation for developing this formalism was to extend previous zero-order approaches (5, 15–17) to the next-order approximation where the homogeneous nature of relevant spin interactions is taken into account. As a result, a theoretical tool could be developed by which the conditions and limitations of multiple-pulse sequences under fast MAS can be understood, in principle.

Based on this, some important conclusions can be drawn. In accordance with the experiment, pronounced decoupling conditions at certain ratios of t_c/τ_R which are expected from zero-order treatment (5, 17) are not found for $t_c < \tau_R$. That is, these conditions seem to be smoothed out by the first-order contributions that are now considered in addition. The implicit presence of these conditions, however, might be responsible for the fact that the quasi-static regime effectively ranges up to a ratio of $t_c/\tau_R = \frac{1}{3}$.

The zero-order synchronization conditions for $t_c > \tau_R$ on the other hand could be confirmed by the above theory. An experimental check was not possible with the semi-windowless pulse sequence used in the experiments but this is not a principal problem. However, there are arguments that such conditions are not very useful for practical applications, where usually different isotropic chemical shifts are present. For the relatively large pulse spacing required for these synchronization conditions, the isotropic chemical-shift evolution can no longer be neglected and the application of average Hamiltonian theory thus becomes problematic. Intuitively spoken, as a result of the off-resonance evolution, the magnetization vector and the pulse directions are no longer in a fixed relationship to each other. Since pulses act only on magnetization components that are perpendicular to them, the magnetization splits into two components after every applied pulse. This results in a rapid decay of off-resonance signal contributions. Only if such an effect can be avoided, for instance, by using suitable compensation strategies along the philosophy outlined in (25–27), might these conditions become useful for line-narrowing experiments.

At present, however, pulsed line-narrowing under MAS seems to be confined to quasi-static conditions. Quasi-static conditions can be realized in form of the classical CRAMPS experiment, where slow MAS is used practically only for the removal of chemical-shift anisotropy and the pulse sequence is a highly efficient, high-order compensated sequence that deals with the dipolar interaction. An alternative realization is the multiple-pulse assisted MAS experiment where quasi-static conditions are achieved by minimizing the cycle time to the extreme and where the averaging of homogeneous interactions relies not only on the pulse sequence but also on fast MAS (15, 16). For such experiments a good compromise must be found between the technical limitations concerning the reduction of the cycle time and the need for high spinning speeds.

Fortunately, the above analysis showed that such experiments are quite forgiving with respect to the ratios t_c/τ_R that are still acceptable. It was found that, even for ratios of up to $t_c/\tau_R = \frac{1}{3}$, satisfactory resolution can be obtained (see Figs. 2 and 4).

Apart from decoupling techniques, the recoupling cases also can be analyzed on the basis of the above treatment. In contrast to decoupling, the zero-order conditions of strongest recoupling (at $t_c/\tau_R = \frac{1}{2}$ and $t_c/\tau_R = 1$) are directly found theoretically and in the experiment. Synchronized recoupling seems to be more easily achieved for homogeneous interactions than decoupling. This can be explained by realizing that for recoupling it is sufficient to reintroduce two-spin correlations, while for efficient decoupling higher spin correlations also must be dealt with.

In conclusion, we have analyzed the conditions and limitations of multiple-pulse experiments under magic-angle spinning. The analysis clearly shows how important a suitable ratio t_c/τ_R is for a successful experiment. It further reveals the principal limitations of the present approaches but leaves room for the development of new methods that are more suitable for MAS experiments. In this connection it should be noted that the multiple-pulse sequences that were already applied under MAS have originally been developed for static conditions. It thus is hoped that progress can be made by new pulse techniques developed directly for use under fast magic-angle spinning.

APPENDIX

We will outline in the following the treatment of a multiple-pulse sequence applied under MAS on the example of the WHH-4 pulse sequence (in the δ-pulse limit) (1). For this, one has to specify $N = 6$ and $\tau_1 = \cdots = \tau_6 = \tau$ in Eqs. [8]–[12]. The toggling frame Hamiltonians $H_{\alpha,m}$ that correspond to these six time intervals are given by the chronologically ordered sequence $[H_{x,m}, H_{y,m}, H_{z,m}, H_{z,m}, H_{y,m}, H_{x,m}]$, where each component contains dipolar and isotropic chemical-shift contributions. For instance, for the x component one obtains for $m = 0$

$$H_{x,0} = H_{x,0}^{CS} = \sum_i \omega_i I_{ix} \qquad [27]$$

and for $m \neq 0$

$$H_{x,m} = H_{x,m}^{D} = \sum_{j>i} \omega_m^{(ij)}(3I_{ix}I_{jx} - \mathbf{I}_i\mathbf{I}_j). \qquad [28]$$

The sums are performed over all nuclear spins of the system, ω_i are the isotropic chemical shifts, and $\omega_m^{(ij)} = \omega_D(ij)b_m^{(ij)}(\theta_{ij}, \varphi_{ij})$ represents the dipolar interactions between the nuclear spins (the dipolar coupling constant and the angular coefficients are defined following the usual conventions) (11). The angles $(\theta_{ij}, \varphi_{ij})$ give the orientation of the dipolar tensor with respect to the rotor frame. In case of ^{1}H spectra (which are our

main interest here) one can neglect the influence of the chemical-shift anisotropy due to fast MAS conditions.

According to Eq. [7] only the $m = 0$ component is present in zero order of the effective Hamiltonian, i.e.,

$$\bar{\mathcal{H}}_{\text{eff}}^{(0)} = \frac{1}{3} \sum_i \omega_i (I_{ix} + I_{iy} + I_{iz}). \qquad [29]$$

The first-order term contains two distinct contributions. The first, $\bar{\mathcal{H}}_0^{(1)}$, corresponds to the zero-order term in the Floquet expansion which consists of Fourier components that represent first-order terms in the Magnus expansion, that is,

$$\bar{\mathcal{H}}_0^{(1)} = \frac{-i}{2t_c} \sum_m \{ [H_{x,m}^D, H_{y,-m}^D] a_m^{xy} + [H_{x,m}^D, H_{z,-m}^D] a_m^{xz}$$
$$+ [H_{y,m}^D, H_{z,-m}^D] a_m^{yz} + [H_{x,m}^D, H_{x,-m}^D] a_m^{xx}$$
$$+ [H_{y,m}^D, H_{y,-m}^D] a_m^{yy} + [H_{z,m}^D, H_{z,-m}^D] a_m^{zz} \}, \qquad [30]$$

where the coefficients are given by

$$a_m^{xy} = [c_m(\tau_6)c_{-m}(\tau_5) + c_m(\tau_6)c_{-m}(\tau_2)$$
$$\quad - c_m(\tau_5)c_{-m}(\tau_1) - c_m(\tau_2)c_{-m}(\tau_1)]$$
$$a_m^{xz} = [c_m(\tau_6)c_{-m}(\tau_4) + c_m(\tau_6)c_{-m}(\tau_3)$$
$$\quad - c_m(\tau_3)c_{-m}(\tau_1) - c_m(\tau_4)c_{-m}(\tau_1)]$$
$$a_m^{yz} = [c_m(\tau_5)c_{-m}(\tau_4) + c_m(\tau_5)c_{-m}(\tau_3)$$
$$\quad - c_m(\tau_4)c_{-m}(\tau_2) - c_m(\tau_3)c_{-m}(\tau_2)]$$
$$a_m^{xx} = [c_m(\tau_6)c_{-m}(\tau_1) + c_{m,-m}(\tau_6) + c_{m,-m}(\tau_1)]$$
$$a_m^{yy} = [c_m(\tau_5)c_{-m}(\tau_2) + c_{m,-m}(\tau_5) + c_{m,-m}(\tau_2)]$$
$$a_m^{zz} = [c_m(\tau_4)c_{-m}(\tau_3) + c_{m,-m}(\tau_4) + c_{m,-m}(\tau_3)], \qquad [31]$$

with $c_m(\tau_j)$ and $c_{m,-m}(\tau_j)$ given by Eqs. [9] and [11]. Taking into account that all τ_j are equal to each other and equal with τ, they can be rewritten as

$$a_m^{xy} = 4i \frac{[\sin(m\omega_R\tau) + \sin(4m\omega_R\tau)][1 - \cos(m\omega_R\tau)]}{(m\omega_R)^2}$$

$$a_m^{xz} = 4i \frac{[\sin(2m\omega_R\tau) + \sin(3m\omega_R\tau)][1 - \cos(m\omega_R\tau)]}{(m\omega_R)^2}$$

$$a_m^{yz} = 4i \frac{[\sin(m\omega_R\tau) + \sin(2m\omega_R\tau)][1 - \cos(m\omega_R\tau)]}{(m\omega_R)^2}$$

$$a_m^{xx} = 2i \frac{\sin(5m\omega_R\tau)[1 - \cos(m\omega_R\tau)]}{(m\omega_R)^2}$$

$$+ \frac{i}{m\omega_R} \left[\tau - \frac{\sin(m\omega_R\tau)}{m\omega_R} \right]$$

$$a_m^{yy} = 2i \frac{\sin(3m\omega_R\tau)[1 - \cos(m\omega_R\tau)]}{(m\omega_R)^2}$$

$$+ \frac{i}{m\omega_R} \left[\tau - \frac{\sin(m\omega_R\tau)}{m\omega_R} \right]$$

$$a_m^{zz} = 2i \frac{\sin(m\omega_R\tau)[1 - \cos(m\omega_R\tau)]}{(m\omega_R)^2}$$

$$+ \frac{i}{m\omega_R} \left[\tau - \frac{\sin(m\omega_R\tau)}{m\omega_R} \right]. \qquad [32]$$

Since the coefficients $a_m^{\alpha\beta}$ are odd functions with respect to the substitution $m \to -m$, i.e., $a_m^{\alpha\beta} = -a_{-m}^{\alpha\beta}$ for each mixed commutator of the form $[H_{\alpha,m}^D, H_{\beta,-m}^D]$, one can introduce in Eq. [30] its symmetric counterpart $[H_{\beta,m}^D, H_{\alpha,-m}^D]$. A further simplification is obtained based on the relationship $\sum_\alpha [H_{\alpha,m}^D, H_{\alpha,-m}^D] = -3[F_m^D, F_{-m}^D]$, where $F_m^D = \sum_{j,k} b_m^{ij}(\theta_{ij}, \varphi_{ij}) \mathbf{I}_j \mathbf{I}_k$ represents the isotropic part (with respect to the spin operators) of the full dipolar Hamiltonian. Taking into account these properties, the relations Eqs. [30] and [32] can be combined into a more concise expression, namely,

$$\bar{\mathcal{H}}_0^{(1)} = \sum_m f_m(\tau) \sum_{\alpha,\beta} A_m^{\alpha\beta}(\tau) \frac{[H_{\alpha,m}^D, H_{\beta,-m}^D]}{2m\omega_R}$$
$$+ g_m(\tau) \frac{[F_m^D, F_{-m}^D]}{2m\omega_R}, \qquad [33]$$

where we have explicitly separated the coefficients

$$A_m^{xy} = A_m^{yx} = [\sin(m\omega_R\tau) + \sin(4m\omega_R\tau)]$$
$$A_m^{xz} = A_m^{zx} = [\sin(2m\omega_R\tau) + \sin(3m\omega_R\tau)]$$
$$A_m^{yz} = A_m^{zy} = [\sin(m\omega_R\tau) + \sin(2m\omega_R\tau)]$$
$$A_m^{xx} = \sin(5m\omega_R\tau)$$
$$A_m^{yy} = \sin(3m\omega_R\tau)$$
$$A_m^{zz} = \sin(m\omega_R\tau), \qquad [34]$$

which depend on the components (α, β) and the functions

$$f_m(\tau) = \frac{2\pi}{3} \frac{1 - \cos(m\omega_R\tau)}{m\omega_R\tau} \qquad [35]$$

and

$$g_m(\tau) = \frac{1}{6} \left(1 - \frac{\sin(m\omega_R\tau)}{m\omega_R\tau} \right), \qquad [36]$$

which are independent of (α, β).

The second contribution, $[\bar{\mathcal{H}}_m^{(0)}, \bar{\mathcal{H}}_{-m}^{(0)}]/2m\omega_R$, represents the first-order term in the Floquet expansion which contains Fourier components that are zero-order in the Magnus expansion. It can be evaluated following exactly the same steps as above and, brought to a similar form as Eq. [33], reads

$$\sum_m \frac{[\bar{\mathcal{H}}_m^{(0)}, \bar{\mathcal{H}}_{-m}^{(0)}]}{2m\omega_R} = \sum_m f_m(\tau) \sum_{\alpha,\beta} B_m^{\alpha\beta}(\tau) \frac{[H_{\alpha,m}^D, H_{\beta,-m}^D]}{2m\omega_R}.$$

[37]

No isotropic term is present here and the values of the (α, β)-dependent coefficients are different from those of Eq. [33], i.e.,

$$B_m^{xy} = B_m^{yx} = \frac{1}{3m\omega_R\tau} \left[\cos(m\omega_R\tau) + \cos(4m\omega_R\tau)\right]$$

$$B_m^{xz} = B_m^{zx} = \frac{1}{3m\omega_R\tau} \left[\cos(2m\omega_R\tau) + \cos(3m\omega_R\tau)\right]$$

$$B_m^{yz} = B_m^{zy} = \frac{1}{3m\omega_R\tau} \left[\cos(m\omega_R\tau) + \cos(2m\omega_R\tau)\right]$$

$$B_m^{xx} = \frac{1}{3m\omega_R\tau} \left[1 + \cos(5m\omega_R\tau)\right]$$

$$B_m^{yy} = \frac{1}{3m\omega_R\tau} \left[1 + \cos(3m\omega_R\tau)\right]$$

$$B_m^{zz} = \frac{1}{3m\omega_R\tau} \left[1 + \cos(m\omega_R\tau)\right].$$

[38]

Now combining both contributions, one finds that the first-order effective Hamiltonian, Eq. [7], is given by Eq. [15]. The synchronization functions $f_m^{\alpha\beta}(\tau)$ result from the sum of the corresponding coefficients A and B and are given by Eq. [18].

ACKNOWLEDGMENTS

REFERENCES

1. J. S. Waugh, L. Huber, and U. Haeberlen, Approach to high-resolution NMR in solids, *Phys. Rev. Lett.* **20,** 180–182 (1968).

2. E. R. Andrew, A. Bradbury, and R. G. Eads, NMR from a crystal rotated at high speeds, *Nature* **182,** 1959 (1958).

3. I. J. Lowe, Free induction decays in rotating solids, *Phys. Rev. Lett.* **2,** 285 (1959).

4. A. E. Bennet, R. G. Griffin, and S. Vega, Recoupling of homo- and heteronuclear dipolar interactions in rotating solids, *in* "NMR, Basic Principles and Progress," Vol. 33, Springer-Verlag, Berlin, 1994.

5. S. Hafner and H. W. Spiess, Advanced solid-state NMR spectroscopy of strongly dipolar coupled spins under fast magic angle spinning, *Concepts Magn. Reson.* **10,** 99–128 (1998).

6. M. Maricq and J. S. Waugh, NMR in rotating solids, *J. Chem. Phys.* **70,** 3300–3316 (1979).

7. C. Filip, S. Hafner, I. Schnell, D. E. Demco, and H. W. Spiess, Solid-state NMR spectra of dipolar-coupled multi-spin systems under fast magic angle spinning, *J. Chem. Phys.* **110,** 423–440 (1999).

8. C. Filip, X. Filip, D. E. Demco, and S. Hafner, Spin dynamics under magic angle spinning by Floquet formalism, *Mol. Phys.* **92,** 757–771 (1997).

9. W. K. Rhim, D. D. Elleman, and R. W. Vaughn, Analysis of multiple pulse NMR in solids, *J. Chem. Phys.* **59,** 3740–3749 (1973).

10. P. Mansfield, M. J. Orchard, D. C. Stalker, and K. H. B. Richards, Symmetrized multipulse nuclear magnetic resonance experiments in solids: Measurement of the chemical-shift shielding tensor in some compounds, *Phys. Rev. B* **7,** 90–105 (1973).

11. U. Haeberlen, High-resolution NMR of solids, *in* "Advances in Magnetic Resonance: Selective Averaging," Academic Press, New York, 1976.

12. R. E. Taylor, R. G. Pembleton, L. M. Ryan, and B. C. Gerstein, Combined multiple pulse NMR and sample spinning: Recovery of ^{1}H chemical shift tensors, *J. Chem. Phys.* **71,** 4541–4545 (1979).

13. G. Scheler, U. Haubenreiser, and H. Rosenberger, High-resolution ^{1}H NMR in solids with multiple-pulse sequences and magic-angle sample spinning at 270 MHz, *J. Magn. Reson.* **44,** 134–144 (1981).

14. S. T. Dec, C. E. Bronnimann, R. A. Wind, and G. E. Maciel, Comparison of the ^{1}H NMR analysis of solids by the CRAMPS and MAS-only techniques, *J. Magn. Reson.* **82,** 454–466 (1989).

15. S. Hafner and H. W. Spiess, Multiple-pulse line-narrowing under fast magic-angle spinning, *J. Magn. Reson. A* **121,** 160–166 (1996).

16. S. Hafner and H. W. Spiess, Multiple-pulse assisted line-narrowing by fast magic-angle spinning, *Solid State NMR* **8,** 17–24 (1997).

17. D. E. Demco, S. Hafner, and H. W. Spiess, Rotation-synchronized homonuclear dipolar decoupling, *J. Magn. Reson. A* **116,** 36 (1995).

18. S. Vega, E. T. Olejniczak, and R. G. Griffin, Rotor frequency lines in the nuclear magnetic resonance spectra of rotating solids, *J. Chem. Phys.* **80,** 4832 (1984).

19. O. Weintraub and S. Vega, Floquet density matrices and effective Hamiltonians in magic-angle-spinning NMR spectroscopy, *J. Magn. Reson. A* **105,** 245–267 (1993).

20. T. Nakai and C. A. McDowell, Application of Floquet theory to the nuclear magnetic resonance spectra of homonuclear two-spin systems in rotating solids, *J. Chem. Phys.* **96,** 3452–3466 (1992).

21. T. O. Levante, M. Baldus, B. H. Meier, and R. R. Ernst, Formalized Floquet theory and its applications to sample spinning in nuclear magnetic resonance, *Mol. Phys.* **86,** 1195–1212 (1995).

22. M. Lee and W. I. Goldburg, Nuclear-magnetic-resonance line narrowing by a rotating rf field, *Phys. Rev. B* **140,** A1261–A1271 (1965).

23. U. Haeberlen and J. S. Waugh, Coherent averaging effects in magnetic resonance, *Phys. Rev.* **175,** 453–467 (1968).

24. M. Hohwy and N. C. Nielsen, Elimination of high order terms in multiple pulse nuclear magnetic resonance spectroscopy: Application to homonuclear decoupling in solids, *J. Chem. Phys.* **106,** 7571–7586 (1997).

25. H. Cho, Off-resonance multiple-pulse dynamics in solid-state NMR spectroscopy: A revised coherence averaging theory analysis, *J. Chem. Phys.* **141,** 164–179 (1999).

26. T. M. Barbara and L. Baltusis, Phase-cycled multiple-window-acquisition, multiple-pulse NMR, *J. Magn. Reson. A* **106,** 182 (1994).

27. H. Cho, Tilted-axis precession and phase-sensitive detection of nuclear magnetization, *J. Magn. Reson. A* **121,** 8–22 (1996).